Hidden images in halftone pictures

Joseph Rosen and Bahram Javidi

A method of concealing an image in a different halftone image is proposed. Continuous-tone levels of the visible images are represented by the area of the halftone dots. However, the hidden image is encoded by the dots' positions inside their cells. Only a spatial correlator with a unique filter function can reveal the hidden image from the halftone picture. The technique and its robustness to noise and distortions are demonstrated. © 2001 Optical Society of America

OCIS codes: 100.2810, 090.1760, 070.2580, 070.4560, 050.1380, 070.4550, 070.6110.

1. Introduction

Halftone coding is a common method of representing continuous-tone images by binary values. In one of many techniques for halftone binarization[1] the various tone levels are translated to the area of binary dots. This method, termed binarization by a carrier,[2] is related to the pulse-width modulation in communication theory. For our purposes it is termed, in an analog fashion, dot-area modulation (DAM). The locations of the dots inside their cells in the halftone picture usually do not represent any information. When the positions of the dots are not uniform from cell to cell, the nonuniformity is actually used to reduce the difference between the original gray-tone image and the resultant binary image as viewed by the detection system.[1] However, from communication theory we know that pulse-position modulation is a common method of representing information that is similar to pulse-width modulation. We propose a different method of encoding visual information in a halftone image independently of the common DAM coding in a way that is similar to pulse-position modulation. This method is naturally termed dot-position modulation (DPM).

The independence of DAM and DPM from each other permits each method to encode a different image in the same halftone picture. However, one cannot see the DPM-encoded image directly by simply observing the halftone picture. The image encoded by the DPM is hidden in the halftone picture, and a specific means of revealing this secret image is needed. This property indicates possible applications of DPM for information security and encryption.[3] In general, this technique can be used as a pictured dot code. On the one hand it is a collection of dots used as a secret code, which can be deciphered only by a special key. On the other hand, unlike other known codes, for example, the common bar code, this code is a picture in the sense that the code itself is a meaningful image, encoded by DAM independently of the hidden image encoded by DPM. Another application might be embedding steganographic information[4,5] in halftone pictures. The ordinary visible image is conventionally encoded by DAM, whereas the steganographic image is encoded by DPM. A possible application for this technique might be, for example, in identification cards.[6] A special halftone photograph of a person on an identification card can show the card holder's picture as usual. However, the same photograph can conceal confidential data such as an image of the person's signature, his or her fingerprint, or some other personal records. The cardholder in this case must be matched to both types of image and to all the rest of the data on the card. Thus counterfeiting of identification cards by a person who resembles the authentic person, or switching of the photographs on their identification cards, without being discovered becomes much more difficult. The steganographic images are revealed by a special key in a particular processor that we discuss next.

Our proposed tool for revealing the hidden image is the well-known two-dimensional (2-D) spatial correlator.[7] The spatial filter of this correlator is the key function that enables the hidden image to appear on

J. Rosen (rosen@ee.bgu.ac.il) is with the Department of Electrical and Computer Engineering, Ben-Gurion University, Beer-Sheva 84105, Israel. B. Javidi is with the Department of Electrical and Computer Engineering, University of Connecticut, U-157, 260 Glenbrook Road, Storrs-Mansfield, Connecticut 06269-2157.

Received 24 October 2000; revised manuscript received 12 March 2001.

0003-6935/01/203346-08$15.00/0

the output plane when the halftone figure is displayed on the correlator input plane. In other words, the hidden image is obtained as the correlation function between the halftone picture and a reference function. The reference function is related to the spatial filter function by a 2-D Fourier transform (FT). Using the correlator has the following advantages:

1. The image reconstruction from the halftone picture is relatively robust to noise. This is so because, for some requirements on the size of the key reference function, the hidden image is memorized globally in all the halftone's dots. This means that every pixel in the output image is obtained as a weighted sum of the entire input picture's dots. Therefore, even if several pixels from the input halftone figure are distorted from their correct values, the output result can still be recognized because of the contributions from the other, nondistorted pixels.
2. The spatial correlator has the property of the shift invariance, which means that, no matter where the halftone image appears at the input plane, the hidden output image is produced on the output plane.
3. The same deciphering system can be implemented as an optical, electrical, or hybrid system. This is so because spatial 2-D correlators can be implemented by the optical VanderLugt correlator,[8] by the hybrid joint-transform correlator,[9] or by a digital computer. The system that we demonstrate in the present study is based on digital computing, although the use of optical correlators is also discussed.
4. When digital correlations are used, it is obvious to use the fast-FT algorithm as a tool for computing the correlations, both in the coding process and in reading the hidden images. Therefore the computation time is relatively short compared with those of other, more general, linear space-variant processors.[10]

2. Encoding of Images in a Halftone Picture

The coding process starts with the data of two images, the visible image $f(x, y)$ and the hidden image $a(\xi, \eta)$. They are defined in different coordinate systems because they are observed in two different planes. $f(x, y)$ is observed on the correlator's input plane; $a(\xi, \eta)$, on its output plane. Because they represent gray-tone images, both functions are real and positive. An additional function is determined once at the beginning of the process and is referred to the key function $H(u, v)$. $H(u, v)$ is the filter function displayed on the spatial-frequency plane, and its inverse FT (IFT) is denoted $h(x, y)$. For reasons of algorithm stability explained below, $H(u, v)$ is a phase-only function of the form $H(u, v) = \exp[i\phi(u, v)]$, where $\phi(u, v)$ is a random function generated by a random-number generator of the computer and is uniformly distributed on the interval $-\pi$ to π. The computational problem is to find the halftone figure that, correlated with the predefined function $h^*(-x, -y)$, yields the hidden output image $a(\xi, \eta)$. The visible image $f(x, y)$ is used as the constraint on the input function. This means that, instead of a meaningless pattern of binary dots in the input, the halftone picture presents the image $f(x, y)$.

The proposed algorithm is separated into two stages. In the first stage we compute a phase function $\exp[i\theta(x, y)]$ of the complex function $g(x, y) = f(x, y) \times \exp[i\theta(x, y)]$. In other words, we are looking for a phase function $\exp[i\theta(x, y)]$ that, when it is multiplied by the image function $f(x, y)$ and passes through the correlator, results in a complex function with a magnitude that is equal to the hidden image $a(\xi, \eta)$. Therefore one can get two independent images $f(x, y)$ in the input plane and $a(\xi, \eta)$ in the output. Both functions are the magnitude of the two complex functions. In the second stage the complex gray-tone function $g(x, y)$ is binarized to a final halftone image. In other words, the phase function $\exp[i\theta(x, y)]$ is embedded in the binary pattern by DPM and the image $f(x, y)$ is encoded by DAM. We next describe the first part of the algorithm; the second stage follows.

As we have mentioned, our goal for the first stage is to find the phase function $\exp[i\theta(x, y)]$ of the input function $g(x, y)$ such that a correlation between $g(x, y)$ and $h^*(-x, -y)$ yields a complex function with the magnitude function $a(\xi, \eta)$. The phase of the output function is denoted $\exp[i\psi(\xi, \eta)]$, and the complex output function is denoted $c(\xi, \eta) = a(\xi, \eta)\exp[i\psi(\xi, \eta)]$. Therefore the output correlation function is

$$\begin{aligned} c(\xi, \eta) &= \{f(x, y)\exp[i\theta(x, y)]\} \otimes h^*(-x, -y) \\ &= \mathrm{IFT}\{\mathrm{FT}[g(x, y)]\exp[i\phi(u, v)]\}, \end{aligned} \tag{1}$$

where $\otimes$ denotes correlation and we recall that the operators FT and IFT are the Fourier transform and the inverse Fourier transform, respectively. From Eq. (1), the input function is given by

$$\begin{aligned} g(x, y) &= \mathrm{IFT}\left\{\frac{\mathrm{FT}[c(\xi, \eta)]}{H(u, v)}\right\} \\ &= \mathrm{IFT}\{\mathrm{FT}[c(\xi, \eta)]\exp[-i\phi(u, v)]\}. \end{aligned} \tag{2}$$

To compute phase function $\exp[i\theta(x, y)]$ we choose to utilize the projection-onto-constraint-sets (POCS) algorithm modified to operate with correlations.[11] This iterative algorithm starts with an initial random function $\exp[i\theta_1(x, y)]$. Then the function $f(x, y) \times \exp[i\theta_1(x, y)]$ is transformed by the correlation described in Eq. (1). The function $c_1(\xi, \eta)$ is transformed backward by use of the inverse correlation defined by Eq. (2). At every iteration in each of the two domains, (x, y) and (ξ, η), the functions obtained are projected onto the constraint sets. In both domains the constraint sets express the expectation of getting the predefined images $a(\xi, \eta)$ at (ξ, η) and $f(x, y)$ at (x, y). The algorithm continues to iterate between the two domains until the error between the actual and the desired image functions is no longer meaningfully reduced.

The constraint on the output plane is defined by the

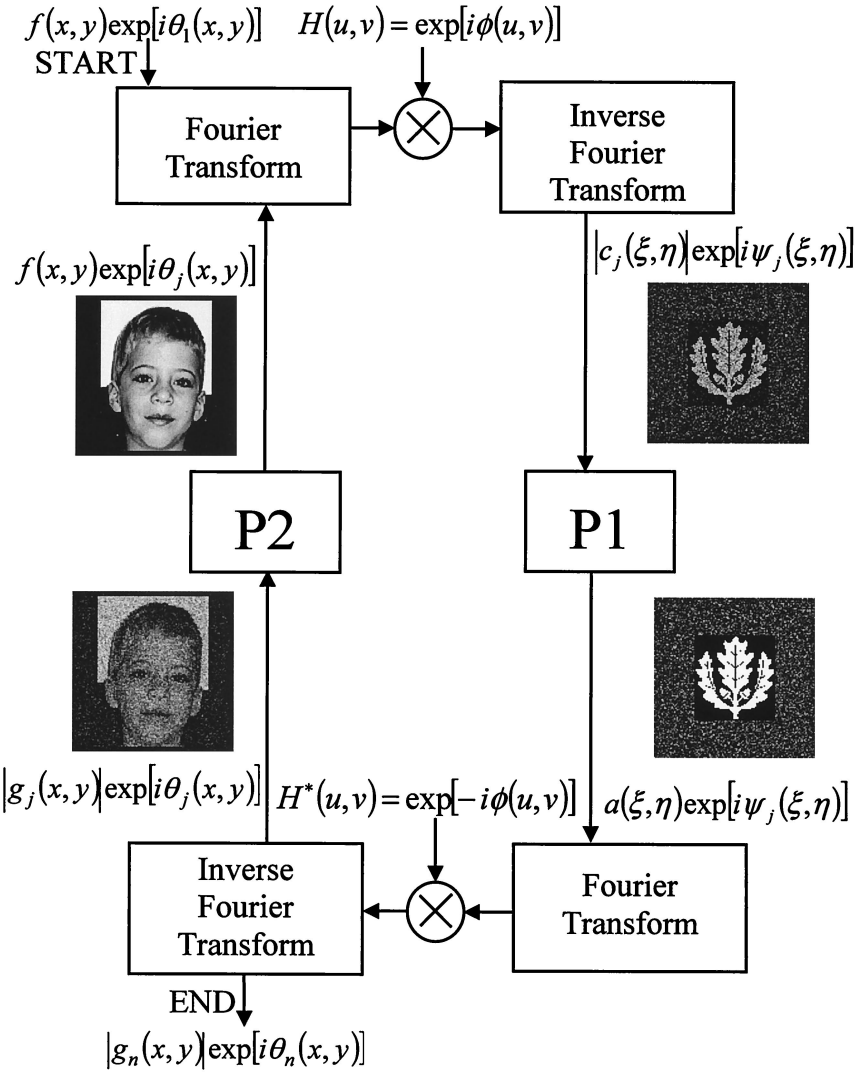

Fig. 1. Block diagram of the POCS algorithm used in the first stage of halftone production.

requirement to obtain the hidden image $a(\xi, \eta)$. Therefore, in the output plane, projection P_1 onto the constraint set at the jth iteration is

$$P_1[c_j(\xi, \eta)] = \begin{cases} a(\xi, \eta)\exp[i\psi_j(\xi, \eta)] & (\xi, \eta) \in W \\ c_j(\xi, \eta) & \text{otherwise} \end{cases}, \tag{3}$$

where $\exp[i\psi_j(x, y)]$ is the phase function of $c_j(\xi, \eta)$ in the jth iteration. W is a window support of the hidden image. The window's area is smaller than, or equal to, the area of the output plane. Similarly, in the input plane, projection P_2 onto the constraint set at the jth iteration is

$$P_2[g_j(x, y)] = f(x, y)\exp[i\theta_j(x, y)], \tag{4}$$

where $\exp[i\theta_j(x, y)]$ is the phase function of $g_j(x, y)$ at the jth iteration. The iteration process is shown schematically in Fig. 1. Note that $H(u, v)$ is chosen only once before the iterations. This $H(u, v)$ becomes part of the correlator, and it is never changed during the iteration process. Moreover, $H(u, v)$ is not in any way related to any of the encoded images and is not any kind of system memory. Therefore $H(u, v)$ does not limit the quantity of image pairs that can be revealed by the same key function. This halftone synthesis can be viewed as a generalization of the Fresnel computer-generated hologram synthesis. In this analogy, $H(u, v)$ acts as a generalized medium between the halftone picture and the reconstructed hidden image, in a fashion similar to that in which the quadratic phase factor represents the free-space medium in the reconstruction of a Fresnel hologram.[12] The function of the medium can be that of a key to expose an image, but the medium does not contain any information about the image and therefore its size does not limit the image capacity that can be utilized by the system.

The convergence of the algorithm to the desired images in the jth iteration is evaluated by two average mean-square errors between the two complex functions, before and after the projections in the two domains. As the phase functions are not changed by

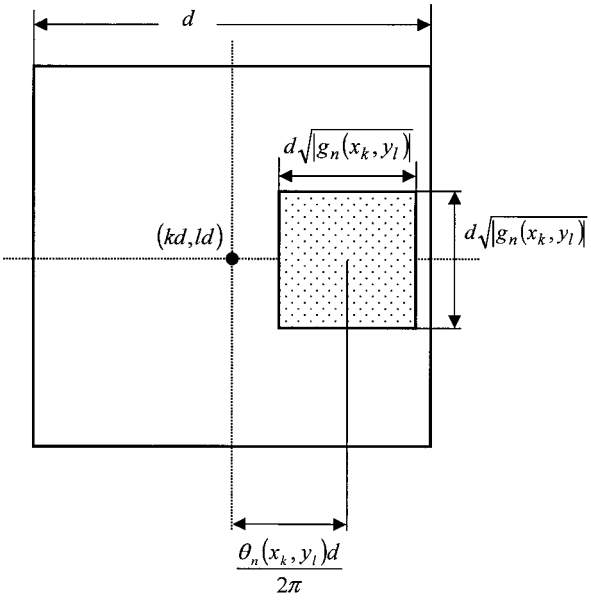

Fig. 2. Schematic of a single cell from an entire halftone picture.

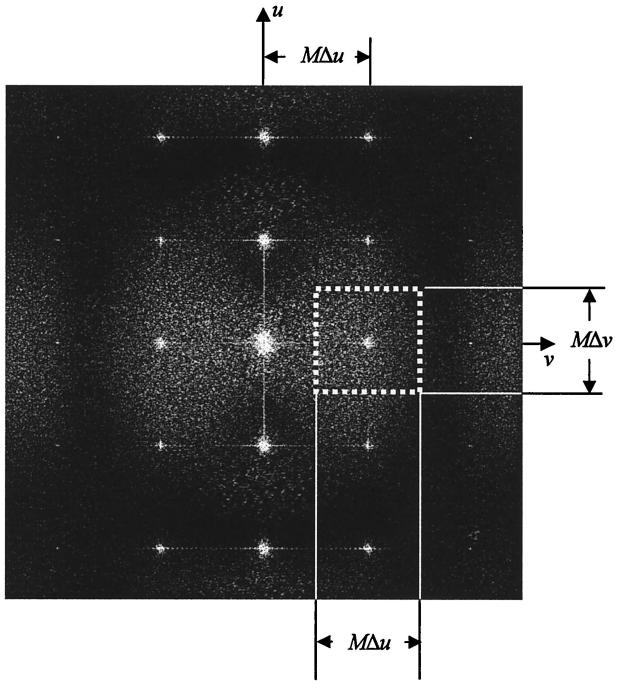

Fig. 3. Spatial spectrum of a typical halftone picture. The area surrounded by the white square is the region that is multiplied by the filter.

the projections, the errors are the average mean square of the difference between magnitudes before and after the projections. The mean-square errors are

$$e_{c,j} = \frac{1}{M_W{}^2} \iint |P_1[c_j(\xi, \eta)] - c_j(\xi, \eta)|^2 \, d\xi d\eta$$
$$= \frac{1}{M_W{}^2} \iint |a(\xi, \eta) - |c_j(\xi, \eta)||^2 \, d\xi d\eta,$$
$$e_{g,j} = \frac{1}{M^2} \iint |P_2[g_j(x, y)] - g_j(x, y)|^2 \, dx dy$$
$$= \frac{1}{M^2} \iint |f(x, y) - |g_j(x, y)||^2 \, dx dy, \qquad (5)$$

where the size of the input planes is $M \times M$ and the size of the window support of the hidden image in the output plane is $M_W \times M_W$. When the reduction rate of these error functions falls below some predefined value, the iterations can be stopped.

As discussed in Ref. 11, there are two conditions to guarantee that these errors will never diverge. First, the correlator should be an energy-conserving operator. This property is inherently achieved if $H(u, v)$ is a phase-only function, as is indeed so in the present case. The second condition is satisfied if, among all the functions that belong to the constraint sets, the two projected functions in the jth iteration, $P_1[c_j(\xi, \eta)]$ and $P_2[g_j(x, y)]$, are the functions closest (by means of the mean-square metric) to the functions $c_j(\xi, \eta)$ and $g_j(x, y)$, respectively. Because the phase distributions are the same before and after the projections in both domains, it is obvious that the second condition is also fulfilled. Therefore the POCS algorithm here can never diverge, and at most the errors may stagnate at some values. Note that the nondiverging feature of the algorithm is the reason to favor phase-only functions as filters in the spatial-frequency domain. The optical realization of the correlator yields another reason to prefer phase-only filters. These filters theoretically do not absorb energy and thus promote maximum system efficiency.

The first stage of the algorithm is terminated in the nth iteration when the correlation between $g_n(x, y)$ and $h^*(-x, -y)$ yields a complex function whose magnitude, it is hoped, is close enough to the hidden image $a(\xi, \eta)$ by means of a relatively small mean-square error. Note that small error values are not guaranteed and depend on the nature of the given images $a(\xi, \eta)$ and $f(x, y)$. The algorithm is terminated before projection P_2, as indicated in Fig. 1. This is so because, in the next stage, the function $g_n(x, y)$ is binarized, an operation that causes the output image to become only an approximation of the desired image. If we chose to terminate the algorithm after projection P_2, the error in image $a(\xi, \eta)$ would be increased, because the magnitude of the correlation between $P_2[g_n(x, y)]$ and $h^*(-x, -y)$ is only an approximation of $a(\xi, \eta)$, and the binarization adds more error.

The goal of the second stage in our process is to convert the complex function $g_n(x, y)$ into a binary function $b(x, y)$. By displaying $b(x, y)$ on the input plane, we should obtain the hidden image in the output of the correlator equipped with the same filter function $H(u, v)$. In the usual halftone binarization, only a single, positive, real gray-tone function is converted into a binary function. However, in the

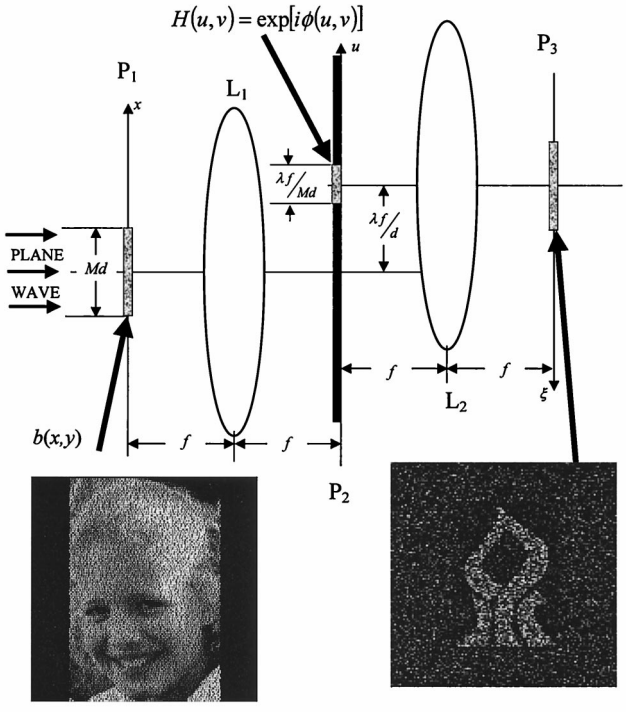

Fig. 4. Optical correlator that can be used to reveal the hidden image in the halftone picture.

present case there are two positive real functions to be encoded, phase $\theta_n(x, y)$ and magnitude $|g_n(x, y)|$, which is close enough to the visible image $f(x, y)$ if $e_{g,n}$ is indeed small. Following computer-generated hologram (CGH) techniques,[13] we propose to encode magnitude $|g_n(x, y)|$ in the conventional way with DAM and phase $\theta_n(x, y)$ with DPM. Every pixel of the complex gray-tone function $g_n(x, y)$ is replaced by a binary submatrix of size $d \times d$. Inside each submatrix there is a dot represented by some binary value, say, 1, on a background of the other binary value, say, 0. The area of the (k, l)th dot is determined by the value of $|g_n(x_k, y_l)|$. The position of the (k, l)th dot inside the submatrix is determined by the value of $\theta_n(x_k, y_l)$. Without loss of generality, we choose the shape of the dot as a square, and each dot is translated only along the horizontal axis. Therefore the expression for the binary halftone image becomes

$$b(x, y) = \sum_{k=-M/2}^{(M/2)B} \sum_{l=-M/2}^{(M/2)B} \operatorname{rect}\left\{\frac{x - d[k + \theta_n(x_k, y_l)/2\pi]}{d[|g_n(x_k, y_l)|]^{1/2}}\right\} \times \operatorname{rect}\left\{\frac{y - ld}{d[|g_n(x_k, y_l)|]^{1/2}}\right\}, \quad (6)$$

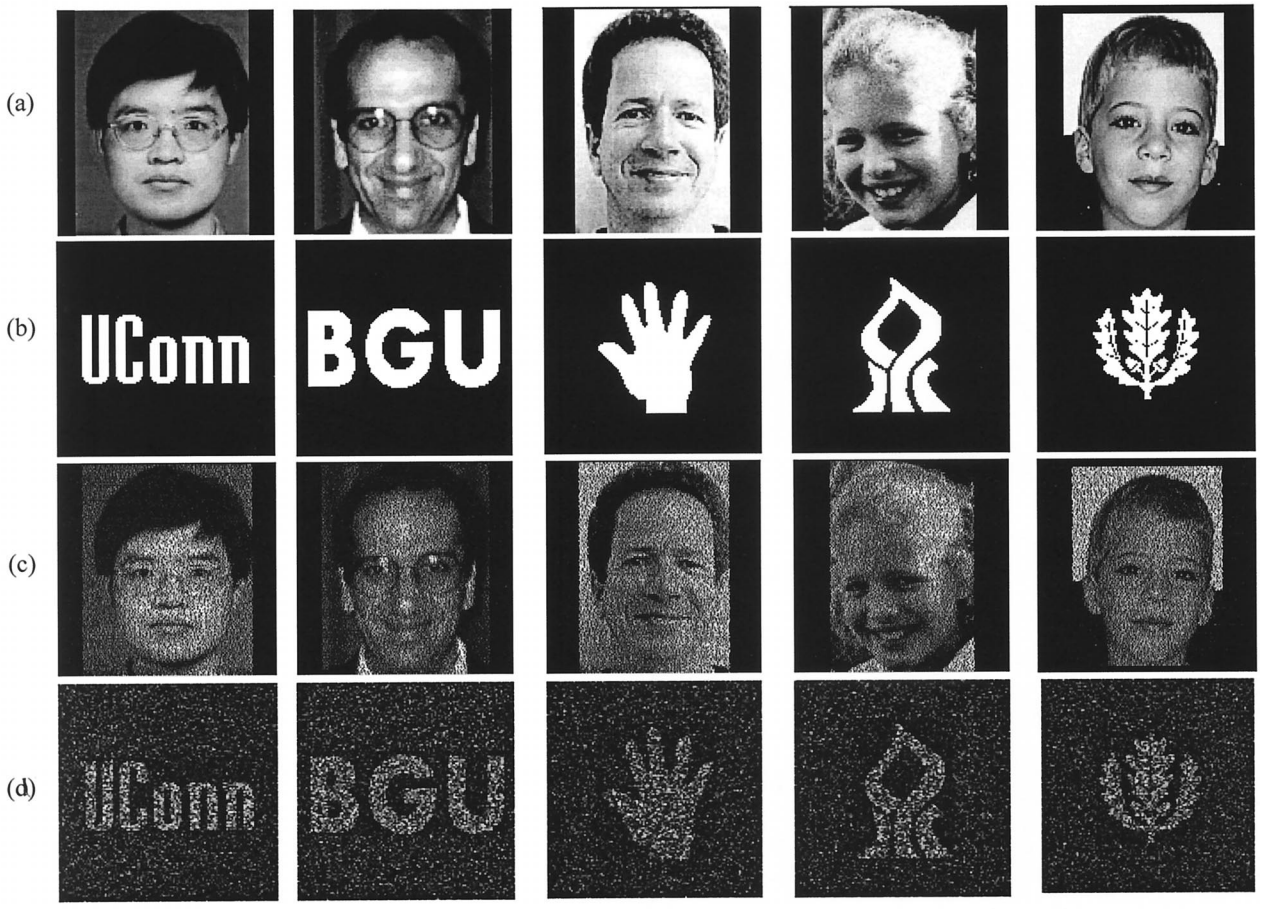

Fig. 5. (a) Original set of gray-tone pictures used as the visible images. (b) Original set of binary pictures used as the hidden images. (c) The resultant halftone images. (d) The hidden images revealed by the correlation between the set in (c) and the key function.

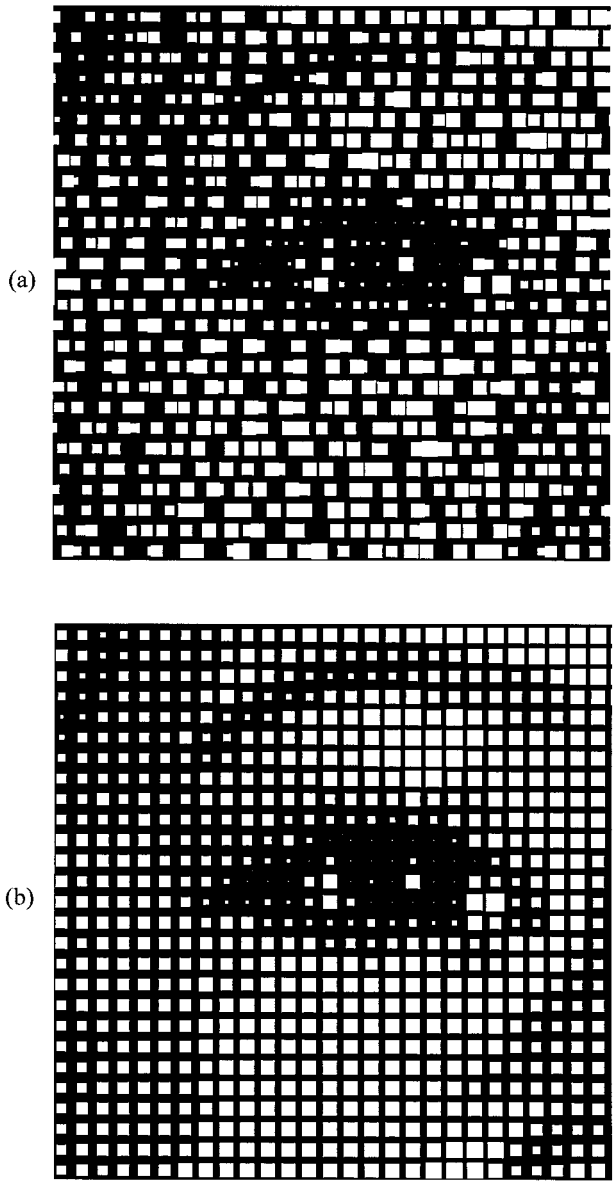

Fig. 6. Enlarged region of a halftone picture (a) with and (b) without dot-position modulation.

where the values of $\theta_n(x, y)$ are defined in the interval $[-\pi, \pi]$, and $0 \le |g_n(x, y)| \le 1$. The function rect(x/a) is defined as 1 for $|x| \le a/2$ and as 0 otherwise. The superscript B in Eq. (6) indicates that the summation is Boolean, such that, if two adjacent rect functions overlap, their sum is 1. A schematic of one of the (k, l)th cells is shown in Fig. 2. $b(x, y)$ is the final halftone binary picture, in which an approximation of the visible image $f(x, y)$ [i.e., $|g_n(x, y)|$] is encoded by the area of the dots. $\theta_n(x, y)$ is embedded into the halftone pattern by the position of the dots, and the hidden image $a(\xi, \eta)$ is exposed at the output plane of the correlator that is described next.

$b(x, y)$ is a 2-D grating, and its Fourier transform is an array of 2-D Fourier orders on the spatial-frequency plane separated by M pixels from one another. An example of a typical spatial spectrum of the grating $b(x, y)$ is depicted in Fig. 3. Following the analysis of the detour-phase CGH,[13] it is possible to show that an approximation of the complex function $G_n(u, v)$[the FT of $g_n(x, y)$] is obtained in the vicinity of the first Fourier-order component. Thus the approximation is expressed as

$$B(u, v) \approx G_n(u, v), \qquad |u - M\Delta u| \le M\Delta u/2, \quad |v| \le M\Delta v/2, \quad (7)$$

where $\Delta u \times \Delta v$ is the size of the pixel in the spatial-frequency plane and $B(u, v)$ is the FT of $b(x, y)$. The fact that the distribution about the first order is only an approximation of $G_n(u, v)$ introduces some error in the reconstructed image. This error is inversely dependent on the number of quantization levels used in the halftone picture. The number of quantization levels is naturally determined by cell size d. Future improvements in the DPM coding may minimize this error in a fashion similar to the evolution of the CGH from the first detour-phase CGH[13] to the more recent and more accurate iterative CGHs.[14] Because the interesting distribution, that is, the approximation of $G_n(u, v)$, occupies only part of the spatial-frequency plane about the first-order component, we isolate this area of $M \times M$ pixels about point $(M, 0)$. Next, the isolated area is multiplied by filter function $H(u, v)$ and inversely Fourier transformed onto the output plane. Because the output distribution is approximately

$$c(\xi, \eta) \approx \mathrm{IFT}[G_n(u, v)H(u, v)], \quad (8)$$

the magnitude of output function $|c(\xi, \eta)|$ is approximately equal to the hidden image, $a(\xi, \eta)$.

The optical version of this correlator is shown in Fig. 4. The halftone figure is displayed on plane P_1 and illuminated by a plane wave. As a result, multiple diffraction orders are obtained on the back focal plane of lens L_1, each at a distance $\lambda f/d$ from its neighbors. The area of the first diffraction order of the size $(\lambda f/Md \times \lambda f/Md)$ is multiplied by the phase-only filter mask $H(u, v)$, whereas the entire spectral area is blocked. The last product is Fourier transformed again by lens L_2 onto plane P_3, where the hidden image is assumed to come into sight. In this scheme we assume that the input halftone picture is a transmission mask that modulates the plane wave. When the halftone picture is printed on regular opaque paper, it has to be recorded first by a digital camera. Then the recorded binary image can be displayed on a spatial light modulator[15] and processed as shown in Fig. 4.

3. Experimental Results with the Digital Correlator

The proposed halftone coding method was examined with a digital correlator. We used five pairs of visible and hidden pictures, as shown in the first two rows of Fig. 5. Originally the visible pictures were gray-tone images of the size of 128×128 pixels, and the hidden pictures were binary images of various sizes (but always smaller than 128×128 pixels).

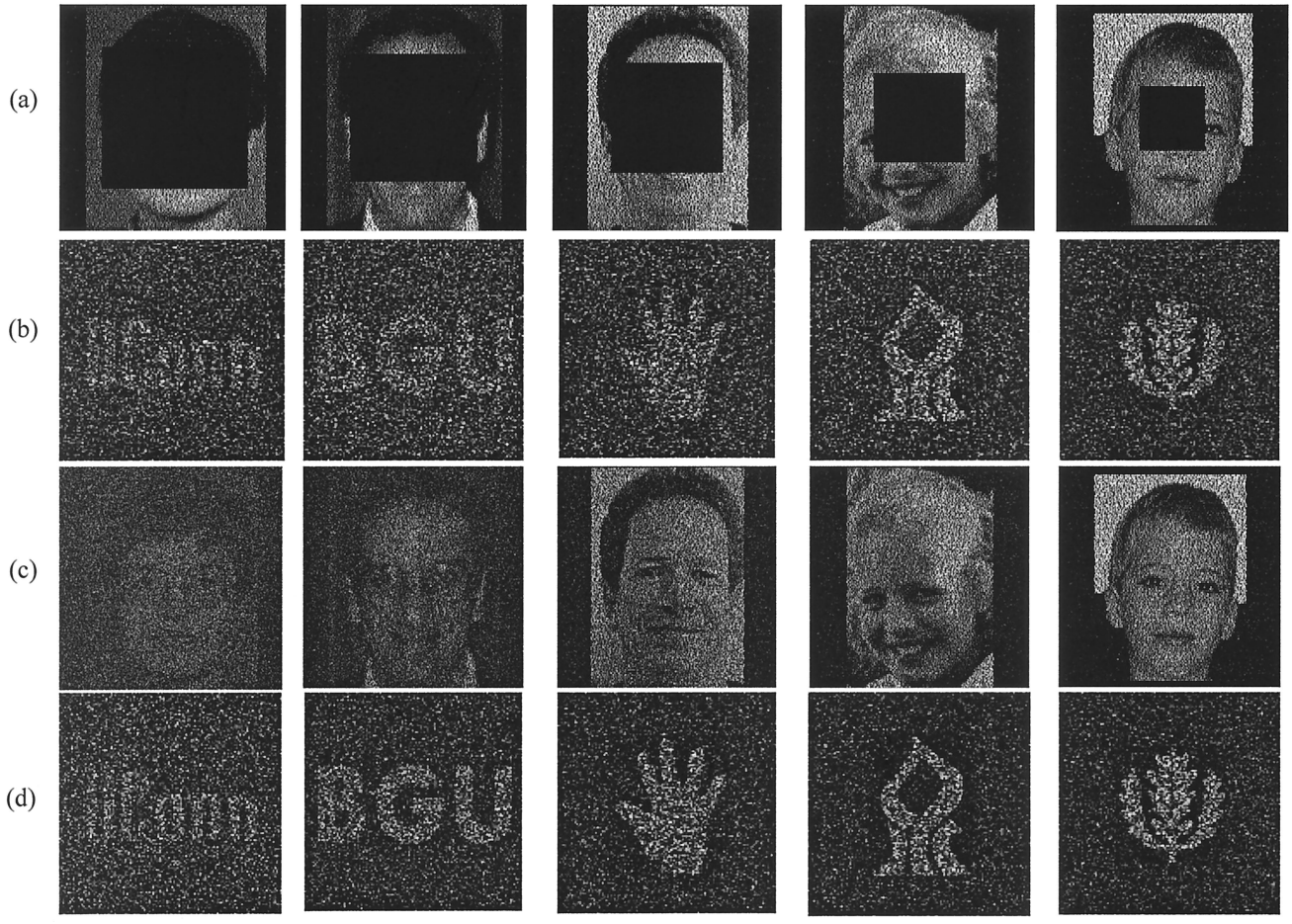

Fig. 7. (a) Set of halftone pictures covered by a zero-valued square with area values that vary from 11% of the picture area at the rightmost figure to 55% at the leftmost figure. (b) Correlation results between the set in (a) and the key function. (c) Set of halftone pictures in which various amounts of their pixel values have been randomly flipped from their original values shown in Fig. 5(c). The number of flipped pixels is varied from 8% at the rightmost figure to 40% at the leftmost figure. (d) Correlation results between the set in (c) and the key function.

The size of each one of the three planes in the POCS algorithm is 128 × 128 pixels. An experiment with all five pairs was performed with the same phase filter $H(u, v)$, for which the phase distribution was generated by the random-number generator of the computer. The POCS algorithm was iterated on average as many as 50 times. Additional iterations have not meaningfully reduced the two errors $e_{c,j}$ and $e_{g,j}$.

After completing the POCS algorithm, we binarized the resultant complex functions $g_n(x, y)$ according to the rule of Eq. (6). The size of each cell in these experiments is 19 × 19 pixels, and consequently the gray-tone image is quantized with 10 levels of magnitude and 19 levels of phase. An enlarged region of one of the halftone figures is shown in Fig. 6(a). For comparison, the same region but without modulation of the dot position are shown in Fig. 6(b). All five halftone pictures with both DAM and DPM coding are depicted in Fig. 5(c). The correlation results with the same $h^*(-x, -y)$ are shown in Fig. 5(d). All five hidden images are recognizable. In principle, we are not limited to choosing gray-tone hidden images rather than binary images as is done in this example. However, as can be seen, the hidden images in Fig. 5(d) are accompanied by a certain level of noise, which naturally becomes more meaningful and destructive for gray-tone images.

The robustness of the method was also examined. As mentioned above, this robustness is achieved because each pixel in the output is obtained as a weighted sum of many input pixels. The exact number of pixels that participate in this summation is equal to the size of $h(x, y)$. In the present study we did not take any action to narrow $h(x, y)$, as was done in the research reported in Ref. 16, for instance. Thus we expect from our system a maximum degree of robustness to noise and distortions. In the first example of distortions illustrated in Fig. 7(a) the five images were covered in the vicinity of their centers with zero-valued squares of an area that varied from 11% to 55% of the original images. The hidden images revealed from these covered halftone figures are shown in Fig. 7(b). The hidden image can still be recognized, even when 55% of the area of the halftone picture is missing. In another example, illustrated

in Fig. 7(c), 8% to 40% of the pixel values of the halftone pictures of Fig. 5(c) were flipped randomly from their original values. The same robust behavior was maintained for this type of noise, as is shown by the correlation results in Fig. 7(d).

4. Conclusions

We have proposed and demonstrated a method of concealing an arbitrary image in a different arbitrary halftone picture. A digital or optical correlator with a unique key filter can recover the hidden image. Every part of the hidden image is concealed globally in all the points of the halftone picture. This feature increases the robustness of the process to noise and distortions.

For future research we believe that different optimization and coding algorithms can significantly reduce the noise and error of both pictures. Also, a clever design of the filter function may extend the distortion-invariance properties of this correlator.

References

1. O. Bryngdahl, T. Scheermesser, and F. Wyrowski, "Digital halftoning: synthesis of binary images," in *Progress In Optics*, E. Wolf, ed. (North-Holland, Amsterdam, 1994), Vol. 33, pp. 389–463.
2. D. Kermisch and P. G. Roetling, "Fourier spectrum of halftone images," J. Opt. Soc. Am. A **65,** 716–723 (1975).
3. B. Javidi, "Securing information with optical technologies," Phys. Today **50**(3), 27–32 (1997).
4. F. A. P. Petitcolas, R. J. Anderson, and M. G. Kuhn, "Information hiding—survey," Proc. IEEE **87,** 1062–1077 (1999).
5. F. Hartung and M. Kutter, "Watermarking digital image and video data," IEEE Signal Proc. Mag. **17**(5), 20–46 (2000).
6. R. L. van Renesse, ed. *Optical Document Security*, 2nd ed. (Artech House, Boston, Mass., 1998), Chap. 18, p. 427.
7. J. W. Goodman, *Introduction to Fourier Optics*, 2nd ed. (McGraw-Hill, New York, 1996), Chap. 8, p. 232.
8. A. B. VanderLugt, "Signal detection by complex spatial filtering," IEEE Trans. Inf. Theory *IT-10,* 139–145 (1964).
9. Ref. 7, Chap. 8, p. 243.
10. Ref. 7, Chap. 8, p. 282.
11. J. Rosen, "Learning in correlators based on projections onto constraint sets," Opt. Lett. **18,** 1183–1185 (1993).
12. O. Bryngdahl and F. Wyrowski, "Digital holography/computer-generated holograms," in Progress In Optics, E. Wolf, ed. (North-Holland, Amsterdam, 1990), Vol. 28, pp. 1–86.
13. A. W. Lohmann and D. P. Paris, "Binary Fraunhofer holograms generated by computer," Appl. Opt. **6,** 1739–1748 (1967).
14. A. K. Jennison, J. P. Allebach, and D. W. Sweeney, "Iterative approaches to computer-generated holography," Opt. Eng. **28,** 629–637 (1989).
15. Ref. 7, Chap. 7, p. 184.
16. Y. Li, K. Kreske, and J. Rosen, "Security and encryption optical systems based on a correlator with significant output images," Appl. Opt. **39,** 5295–5301 (2000).